# Low Temperature Emission Spectra of Individual Single-Walled Carbon Nanotubes: Multiplicity of Subspecies within Single-Species Nanotube Ensembles

H. Htoon, M. J. O'Connell, P. J. Cox, S. K. Doorn, and V. I. Klimov*

*Chemistry Division, Los Alamos National Laboratory, Los Alamos, New Mexico 87545, USA*

(Received 8 February 2004; published 8 July 2004)

Low-temperature photoluminescence (PL) studies of individual semiconducting single-walled carbon nanotubes reveal ultranarrow peaks (down to 0.25 meV linewidths) that exhibit blinking and spectral wandering. Multiple peaks appear within bands previously assigned to nanotubes of certain chiralities, indicating the existence of numerous subspecies within single-chirality specimens. The sharp PL features show two types of distinctly different shapes (symmetric versus asymmetric) and temperature dependences (weak versus strong), which we attribute to the presence of unintentionally doped nanotubes along with undoped species.

DOI: 10.1103/PhysRevLett.93.027401 PACS numbers: 78.67.Ch, 78.55.–m, 78.66.Tr

Single-walled carbon nanotubes (SWNTs) represent a novel class of one-dimensional (1D) objects that have been considered promising building blocks for electronic and optical nanodevices [1]. Despite significant recent progress in their fabrication [2,3], currently available SWNT samples are still highly polydisperse and contain both semiconducting and metallic species with a wide range of diameters and lengths. Because of effects of quantum confinement, the electronic structure of SWNTs exhibits a strong dependence on the tube diameter. This diameter is uniquely related to the SWNT structure by two indices $n$ and $m$ that define the chiral "rollup" vector on a 2D graphene sheet. The species for which $(n - m)$ is divisible by three are metallic or semimetallic, while the others are semiconducting.

Room-temperature (RT) studies of photoluminescence (PL) [4,5] and PL excitation spectra [6–8] of nanotube solutions allowed an assignment of distinct spectroscopic features observed for mixed SWNT ensembles to more than 30 semiconducting species characterized by different $(n, m)$ structures. Recent RT PL measurements of individual nanotubes [9] further revealed some heterogeneities within these "single-species" $(n, m)$ subensembles tentatively attributed to structural/chemical defects and/or fluctuations in the local environment. Significant thermal broadening ($>20$ meV) of RT spectra, however, obscures intrinsic, "nonthermal" line shapes of optical transitions and small static and dynamic variations in PL typical for individual nanoscale objects. In order to reduce the thermal contribution to transition linewidths and to obtain more direct information on SWNT electronic properties, here we perform low-temperature PL studies of individual nanotubes. These studies reveal sharp spectral features with sub-meV homogeneous linewidths that show blinking and spectral wandering, the behaviors typical for individual inorganic [10,11] and organic [12,13] chromophores. The line positions are distributed continuously within single-species bands, indicating the existence of numerous nanotube subspecies within $(n, m)$ subensembles. Further, we observe two distinctly different line shapes (symmetric versus asymmetric), which we attribute to the presence of unintentionally doped SWNTs along with undoped species. While undoped nanotubes produce symmetric "excitonic" lines, the emission of doped nanotubes is characterized by significant asymmetry due to the effect of the Fermi-edge singularity [14] that has been previously observed in metals [15] and doped semiconductors [16,17].

For these studies, we prepare dilute submonolayer samples by dispersing micelle-wrapped SWNT solutions [4] onto crystalline quartz substrates. The samples contain short (average length ~200 nm) SWNTs of various species. A continuous-flow, liquid-He cryostat is used to control the sample temperature within the range of 4 to 60 K. The samples are excited at 532 nm by the output of a continuous-wave frequency-doubled Nd:YAG laser. The size of the excited spot on the sample is 50–80 $\mu$m in diameter. The PL is collected by a microscope objective (numerical aperture 0.6 and 40× magnification) and imaged onto the entrance slit of an imaging spectrometer. The spectrally dispersed images are recorded using a liquid-nitrogen-cooled charge coupled device with integration times from tens of seconds to a few minutes.

Figure 1(a) shows a spectrally dispersed image of approximately 50 nanotubes (sample temperature $T = 4$ K). The spectral peaks cluster into four groups that roughly correspond to RT PL bands [Fig. 1(b), top] assigned previously [6,7] to SWNT species with chiral indices (6, 4), (9, 1), (8, 3), and (6, 5). A histogram [Fig. 1(b), bottom] of 150 PL peaks observed in five different images similar to Fig. 1(a) shows the spectral distribution that closely follows that observed in the ensemble spectra of a solution sample, indicating that our film preparation procedures do not significantly affect the electronic properties of the nanotubes.

An interesting observation is that while some nanotubes exhibit quite stable emission with regard to both the

  

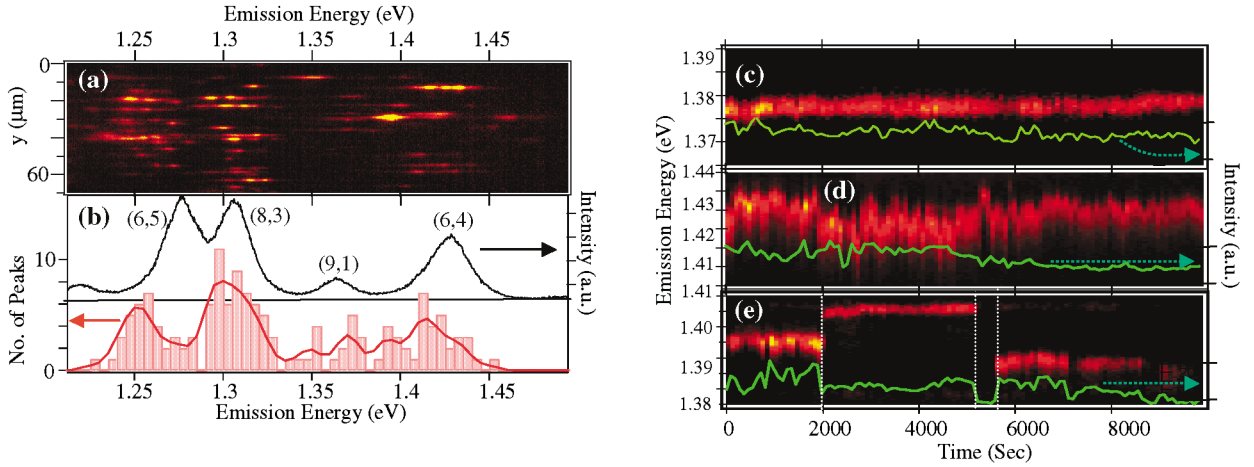


FIG. 1 (color). (a) Spectrally dispersed image of SWNTs recorded at 4 K. Bright horizontal line fragments represent the emission spectra of individual nanotubes. Vertical displacement ($y$) of these lines is determined by the position of the tubes along the entrance slit of the spectrometer. (b) Upper panel: a RT spectrum of the SWNT mixture in solution. Lower panel: a histogram showing the distribution of emission energies of spectral peaks recorded for 150 SWNTs prepared as dilute films [the data were collected from five images similar to that shown in panel (a)]. (c)–(e) These images are examples of three different "fluctuation" behaviors observed for individual nanotubes (see text for details). The false color represents the emission intensity and the 2D image shows the temporal evolution of the spectral position. The green traces at the bottom of each panel show the temporal behavior of the integrated PL intensity.

intensity and the spectral position [green trace and false color image in Fig. 1(c)], there are a number of nanotubes for which both the intensity and the spectral maxima fluctuate quite significantly during the observation time. In our samples we find two types of fluctuation behavior illustrated by examples in Figs. 1(d) and 1(e). The tube in Fig. 1(d) shows continuous, rapid changes in both the PL intensity and the band position (up to 20 meV variations). On the other hand, the tube in Fig. 1(e) is characterized by PL that exhibits random "off/on" switching (PL intermittency) as well as sudden "jumps" in the PL peak position. One can see that this second type of behavior shows clear correlations between PL intermittency and spectral line wandering; namely, the switching in PL intensity is accompanied by jumps in the emission energy.

PL blinking and spectral wandering (as well as correlations between these two processes) have previously been observed for organic and inorganic chromophores [10–13] characterized by both zero-dimensional (semiconductor nanocrystals) and one-dimensional (conjugated polymers) densities of states, for which they have been often explained in terms of interactions with fluctuating environment. These effects have also been considered signatures of emission that arise from an individual chromophore [10–13] and not from a chromophore ensemble. In the case of nanotube samples, these behaviors confirm that the observed PL signals are indeed from single nanotubes but not from, e.g., SWNT bundles.

In order to classify spectroscopic features of low-temperature single nanotube emission, we have analyzed information obtained for 150 individual SWNTs. The right-hand inset of Fig. 2 displays the distribution of line widths [measured as a full width at a half maximum (FWHM)] for all 150 nanotubes. This histogram gives an average linewidth of ~4 meV, though lines as narrow as 0.25 meV are also observed (left-hand inset of Fig. 2). To emphasize a dramatic difference in widths of the ensemble single-species spectrum and the spectra of individual nanotubes, in Fig. 2 we compare the RT PL band nominally attributed to the (8, 3) SWNT species with

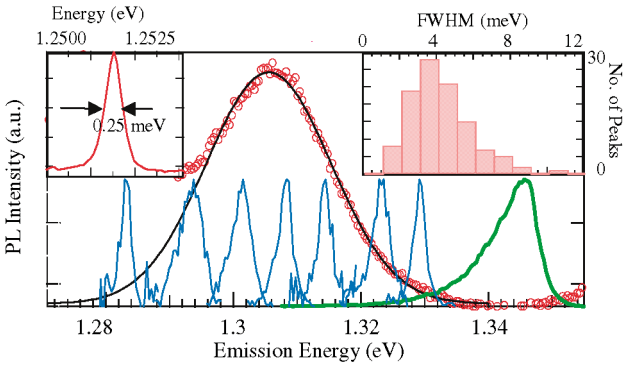


FIG. 2 (color). An expanded view of the RT PL band (a solution sample) corresponding to the (8, 3) nanotube structure (red circles) fit to a Gaussian (black line). This band is compared with narrow symmetric (blue) and asymmetric (green) lines of individual nanotubes that are observed in approximately the same spectral range. Left inset: An example of a narrow symmetric line of a single SWNT that has a 0.25 meV width (derived by taking into account the spectrometer spectral response function). Right inset: Distribution of peak widths derived from the analysis on spectra of 150 individual nanotubes.

spectra of eight single nanotubes that fall into the same spectral range. This comparison indicates that a single-species spectrum can be decomposed into a large number of subspecies spectra that differ not only in spectral positions and widths, but also in shapes. We can classify the single-nanotube spectra into two groups. One group is characterized by relatively narrow linewidths (FWHM $<$ 5 meV) and a symmetric spectral shape. The other group exhibits a broader spectrum (FWHM $>$ 5 meV) that has a pronounced asymmetric shape with a steep, high-energy slope and a longer tail on the low-energy side. Both types of spectra do not show any significant dependence on pump power (varied by more than 2 orders of magnitude; see Figs. 3(a) and 3(b)], and they are observed within all four single-species bands studied in our experiments.

We also study the temperature dependence of nanotube line shapes. These studies indicate that the sample temperature has quite a different effect on symmetric and asymmetric PL peaks [Figs. 3(c) and 3(d)]. While both the shape and width of the symmetric lines are essentially

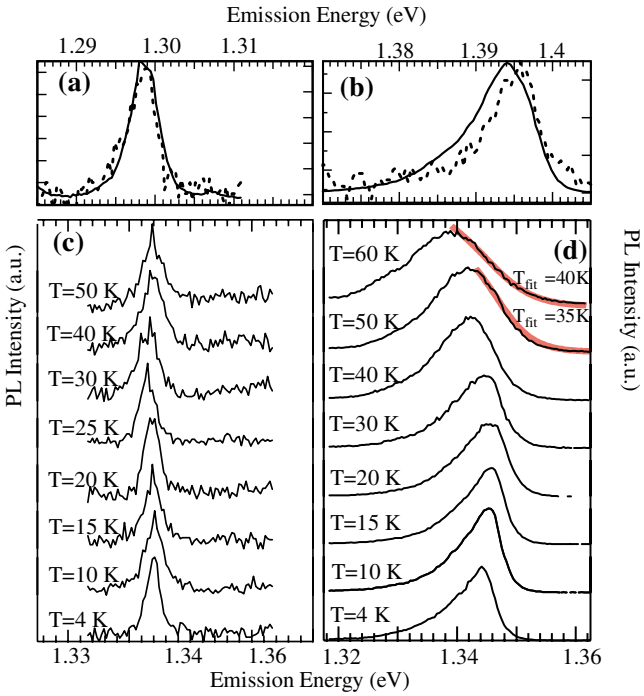


FIG. 3 (color). Examples of symmetric (a) and asymmetric (b) PL spectra of two individual SWNTs taken at low (8.5 W cm$^{-2}$, dashed lines) and high (1.5 kW cm$^{-2}$, solid lines) pump intensities; these data indicate that the contribution from high pump-intensity effects to observed spectral widths is negligible. The temperature dependence observed for symmetric (c) and asymmetric (d) PL spectra. While the symmetric peaks show weak temperature dependence, the asymmetric peaks are characterized by pronounced thermal broadening on their high-energy side. As expected for the FES effect, the high-energy side of the asymmetric spectra recorded at 50 and 60 K can be closely fit (red solid lines) assuming the Fermi distribution of carriers.

independent of temperature in the range of 4 to 60 K, the asymmetric spectra show significant thermal broadening. This broadening primarily affects the steep, high-energy slope of the spectra, making initially asymmetric lines almost symmetric at higher temperatures.

First, we examine the nature of the symmetric lines. The fact that they show only a very weak dependence on the temperature indicates that this type of emission is likely not due to radiative recombination of free electron hole pairs, because the latter would produce PL with a temperature-dependent linewidth, reflecting the width of the thermal distribution of charge carriers within 1D conduction and valence bands. A possible alternative explanation would involve the emission from atomiclike electron-hole bound states (1D excitons) formed due to the Coulombic attraction between oppositely charged carriers [18]. Because of a translational 1D motion, excitons also have a continuous distribution of energies that is dependent upon the sample temperature. However, the momentum and energy conservation laws that govern the process of light emission allow radiative recombination only for a small portion of excitons from a thermally broadened ensemble, which results in a narrow emission line even at relatively high sample temperatures.

The observed distribution in positions of the narrow excitonic lines is likely a result of a different degree of localization of 1D excitons in local potential minima, which could result from structural defects or impurities in the nanotubes [19,20]. In addition, a nonuniform local electrostatic environment could also lead to a "variable" line shift due to the Stark effect [11,13]. Recent studies of the effect of the surfactant on PL from SWNT solution samples also indicate a strong sensitivity of optical transitions to changes in local environment [4,21]. The observed variations in the exciton linewidths are likely also of "extrinsic" origin and may result, e.g., from the tube-to-tube variations in the defect-related scattering rates.

To explain the existence of wide, asymmetric line shapes we invoke the effects of doping. Although our SWNTs are not doped intentionally, earlier studies have shown that, for example, exposure to different types of gases could lead to doping of at least some of the nanotubes in the ensemble [22–24]. Unintentional dopants can also be introduced during different processing steps (e.g., sonication). From previous studies of 2D and 1D semiconductors [16,17], it is well known that at intermediate levels of doping (before the onset of strong screening of the Coulomb potential) a hole photogenerated in the valence band (we consider here the *n*-type doping as an example) can form a so-called Mahan exciton due to its interactions with a Fermi sea of conduction-band electrons [14]. The properties of this exciton are strongly affected by multiparticle interactions that lead, in particular, to the Fermi-edge singularity (FES) effect, which is manifested as a strong increase in absorption and emission intensities at the position of the Fermi level

($\varepsilon_F$) [14]. FES is also associated with a specific asymmetric shape of the emission line that is characterized by a sharp high-energy slope at the Fermi edge and a relatively slow drop on the low-energy side that is observed as a PL tail that extends from the Fermi edge to the band edge. The FES effect was first discovered in x-ray absorption spectra of metals [15] and later was also observed in doped 2D semiconductor quantum wells [16] as well as in 1D quantum wires [17]. It was found that due to the reduced screening of the Coulomb interactions, the FES effect is significantly enhanced in 1D systems compared to semiconductors of higher dimensionality [16], indicating that its occurrence in 1D SWNTs is quite feasible. Furthermore, the symmetric nature of the conduction and valance bands of SWNTs [1] suggests that the FES effect is equally probable in both *p*- and *n*-type SWNTs.

FES theory predicts a power law divergence in the emission intensity at the Fermi edge at 0 K. At nonzero temperatures, the Fermi tail of the carrier distribution gives rise to thermal broadening of the emission spectrum that is particularly well pronounced for the sharp high-energy side of the spectrum. Both the shape and the temperature dependence of individual nanotubes that produce asymmetric PL lines are consistent with those expected for the FES effect. In particular, the thermal broadening of the high-energy side of the PL peak can be well described in terms of the carrier Fermi distribution as indicated by the fits in two top spectra of Fig. 3(d). To further quantify our "FES nanotube" model, we estimate the dopant concentration required to produce the observed linewidths of asymmetric spectral peaks. These concentrations are of the order of $\sim 10^6\ \mathrm{cm}^{-1}$, which corresponds to only one impurity atom per several thousand carbon atoms. This doping level can easily be produced unintentionally during synthesis and/or processing.

We have also considered the possibility of a more traditional explanation of the PL band asymmetry in terms of a phonon-assisted emission producing a low-energy PL tail. However, such an explanation is not consistent with the fact that in our studies of PL intermittency we observe that the fluctuations in the nanotube emission intensity are not accompanied by changes in the PL spectral shape. On the other hand, previous studies of individual nanocrystals, for example, indicate strong changes in the relative intensity for different components of the same phonon progression due to fluctuations in the electron-phonon coupling strength.

In conclusion, we have performed low-temperature PL studies of individual SWNTs. We observe ultranarrow ($<1$ meV) peaks that exhibit blinking and spectral wandering. These sharp features show a wide distribution of positions and widths normally hidden by thermal broadening in room-temperature PL spectra. Specifically, multiple peaks are found within bands previously attributed to certain ($n, m$) species, indicating the existence of numerous subspecies within nominally single-chirality specimens. The analysis of the PL spectral shapes and temperature dependences indicates that one source causing this heterogeneity may be unintentional doping, which can strongly modify the emission spectra of doped tubes through the FES effect.

This work was supported by Los Alamos LDRD Funds and the Chemical Sciences, Biosciences, and Geosciences Division of the Office of Basic Energy Sciences, Office of Science, U.S. Department of Energy.

*To whom correspondence should be addressed.
Email address: Klimov@lanl.gov

[1] *Carbon Nanotubes: Synthesis, Structures, Properties, and Applications*, edited by M. S. Dresselhaus, G. Dresselhaus, and Ph. Avouris (Springer, Berlin, 2001).
[2] C. L. Cheung, A. Kurtz, H. Park, and C. M. Lieber, J. Phys. Chem. B **106**, 2429 (2002).
[3] R. Krupke, F. Hennrich, H. v. Lohneysen, and M. M. Kappes, Science **301**, 344 (2003).
[4] M. J. O 'Connell *et al.*, Science **297**, 593 (2002).
[5] J. Lefebvre, Y. Homma, and P. Finnie, Phys. Rev. Lett. **90**, 217401 (2003).
[6] S. M. Bachilo *et al.*, Science **298**, 2361 (2002).
[7] R. B. Weisman and S. M. Bachilo, Nano Lett. **3**, 1235 (2003).
[8] S. Lebedkin , F. Hennrich, T. Skipa, and M. M. Kappes, J. Phys. Chem. B **107**, 1949 (2003).
[9] A. Hartschuh, H. N. Pedrosa, L. Novotny, and T. D. Krauss, Science **301**, 1354 (2003).
[10] S. A. Empedocles, D. J. Norris, and M. G. Bawendi, Phys. Rev. Lett. **77**, 3873 (1996).
[11] R. G. Neuhauser *et al.*, Phys. Rev. Lett. **85**, 3301 (2000).
[12] D. S. English, A. Furube, and P. F. Barbara, Chem. Phys. Lett. **324**, 15 (2000).
[13] W. E. Moerner and M. Orrit, Science **283**, 1670 (1999).
[14] G. D. Mahan, *Many-Particle Physics* (Plenum, New York, 1981), pp. 743–775.
[15] G. D. Mahan, in *Solid State Physics*, edited by H. Ehrenreich, F. Seitz, and D. Turnbull (Academic, New York, 1974), Vol. 29, pp. 75–138.
[16] M. S. Skolnick *et al.*, Phys. Rev. Lett. **58**, 2130 (1987).
[17] F. Calleja *et al.*, Surf. Sci. **263**, 346 (1992).
[18] C. L. Kane and E. J. Mele, Phys. Rev. Lett. **90**, 207401 (2003); O. J. Korovyanko *et al.*, *ibid.* **92**, 017403 (2004); T. Ando, J. Phys. Soc. Jpn. **66**, 1066 (1997).
[19] D. L. Carroll *et al.*, Phys. Rev. Lett. **78**, 2811 (1997).
[20] H. J. Choi, J. Ihm, S. G. Louie, and M. L. Cohen, Phys. Rev. Lett. **84**, 2917 (2000).
[21] V. C. Moore *et al.*, Nano Lett. **3**, 1379 (2003).
[22] J. Kong *et al.*, Science **287**, 622 (2000).
[23] S. Peng and K. J. Cho, Nanotechnology **11**, 57 (2000).
[24] S. H. Jhi, S. G. Louie, and M. L. Cohen, Phys. Rev. Lett. **85**, 1710 (2000).